When Gold and Silver Differ: Interactions of N-Heterocyclic Carbenes with Noble Metal Surfaces

Aruna Chandran,[1,‡] Shayanta Chowdhury,[1,‡] Gurkiran Kaur,[2] Gaohe Hu,[3] Nathaniel L. Dominique,[1] Lasse Jensen,[3*] David M. Jenkins,[2*] Jon P. Camden[1*]

1 Department of Chemistry and Biochemistry, University of Notre Dame, Notre Dame, IN 46556, United States
2 Department of Chemistry, University of Tennessee, Knoxville, TN 37996, United States
3 Department of Chemistry, The Pennsylvania State University, University Park, PA 16802, United States

***Correspondence to:**
Lasse Jensen
Department of Chemistry
The Pennsylvania State University
University Park, Pennsylvania 16802
jensen@chem.psu.edu

David M. Jenkins
Department of Chemistry
University of Tennessee, Knoxville
Knoxville, TN 37996
djenki15@utk.edu

Jon P. Camden
Department of Chemistry and Biochemistry
University of Notre Dame
Notre Dame, Indiana 46556
jon.camden@nd.edu

‡ Aruna Chandran and Shayanta Chowdhury are equally contributing first authors.

METHODS

EXPERIMENTAL METHODS

Materials. The standard isopropyl winged NHC-CO_2 adduct and the nitrile backboned CO_2 adduct were synthesized according to previously reported procedures.[1] HPLC grade methanol (>99.9%) was purchased from Sigma Aldrich (St. Louis, MO, USA). Concentrated H_2SO_4, 30% H_2O_2, and reagent alcohol (89.5-91.5% ethanol, 4.0-5.0% methanol, and 4.5-5.5% isopropanol) were purchased from VWR (Radnor, PA, USA). The Barnstead system from Thermo Fisher (Waltham, Massachusetts, US) was used to prepare Ultrapure water (18 MΩ).

Substrate Preparation. Silver and gold film-over-nanosphere (AgFON, AuFON) SERS active substrates were prepared using a modified method from a previous report.[2] Glass slides were first cleaned by immersion in freshly prepared piranha acid solution (4:1 concentrated H_2SO_4 to 30% H_2O_2) for 60 minutes. Piranha acid solution must be prepared immediately before use and should not be stored. Any remaining solution should be properly disposed of after use. The cleaned mirrors, after 60 minutes, were rinsed with ultrapure water and reagent alcohol and then dried under nitrogen. A monolayer of 600 nm (diameter) polystyrene beads was assembled at the interface until a compact film was formed and subsequently transferred onto the cleaned glass slides. The polystyrene-coated glass slides were mounted in a physical vapor deposition (Nano36, Kurt J. Lesker, Jefferson Hills, PA, USA) chamber equipped with a quartz crystal microbalance and deposited with a 5 nm chromium adhesion layer followed by ~200 nm of silver or gold. Flat silver and gold mirrors were prepared separately by depositing 5 nm of chromium (as an adhesion layer) and 100 nm of silver or gold onto piranha acid-etched glass slides using the same physical vapor deposition system. Thermal evaporation was performed at a base pressure of ~10^{-6} torr. The mirror substrates were rinsed with reagent-grade alcohol and water, and then dried under nitrogen. Prior to NHC deposition, substrates were rinsed with reagent alcohol followed by HPLC-grade methanol.

Free Carbene Deposition Method. NHC monolayers were prepared via the free carbene method, previously reported in the literature.[3] Free carbene was generated by adding 1,3-

diisopropyl benzimidazolium hexafluorophosphate, (**1**-H)PF_6, (0.100 g, 0.287 mmol, 1 eq) to 10 mL of THF in a 20 mL scintillation vial, followed by KO*t*Bu (0.032 g, 0.287 mmol, 1eq) inside a glove box. After 30 minutes of stirring, the solution was filtered through a Celite pad. Two drops of this free carbene solution in THF were then deposited onto a clean Ag mirror. The vial was allowed to stand for 10 minutes before being removed from the glovebox. The Ag mirror was then washed with methanol (3 x 5 mL) followed by acetone (3 x 10 mL) and dried under N_2 stream.

Methanolic Deposition of NHC on Ag and Au substrates at 58 °C. The substrates were rinsed with reagent alcohol, followed by HPLC-grade methanol. The substrates were subsequently immersed in a 10 mM methanolic solution of the NHC precursor and incubated at 58 °C for 24 hours. The substrates were then rinsed with reagent alcohol after the deposition.

Surface-enhanced Raman Spectroscopy (SERS). SERS measurements were collected on a custom-built Raman setup[4-6] using a 633 nm HeNe laser (Thorlabs) and a laser power of 1 mW (measured at the objective using LaserCheck power meter by Coherent). The laser beam was focused onto the sample using an inverted microscope (Nikon) with a 10x objective lens. The scattered light was collected through the same objective and passed through a Rayleigh rejection filter (Semrock), which was then directed to the spectrometer (Princeton Instruments Acton). Scattered radiation was detected using a liquid nitrogen-cooled CCD detector (Princeton Instruments). All spectra were baseline-corrected, normalized to the most intense peak, and then averaged together to produce the final spectra shown in this work.

Laser Desorption/Ionization Mass Spectrometry (LDI-MS). LDI-MS measurements were collected using a Bruker UltrafleXtreme MALDI-TOF-TOF instrument equipped with a frequency tripled Nd:YAG laser (355 nm). Silver mirrors were mounted on a polished steel sample target using copper tape and a custom 3D-built PEEK sample adapter. All mass spectra were acquired in positive ion mode with the reflectron in operation. The maximum laser power was expressed as a percentage relative to the highest achievable

power with a global attenuator offset of approximately 35%. For each spectrum, a minimum of 2000 laser shots was accumulated at 100% (maximum) laser power. The instrument was calibrated using Ag clusters, following the method of Havel.[7]

X-Ray Photoelectron Spectroscopy. XPS measurements of silver and gold mirror samples were carried out using a PHI VersaProbe II surface analysis instrument from Physical Electronics (Chanhassen, MN) equipped with a monochromatic Al Kα X-ray source (photon energy = 1486.6 eV). High-resolution spectra were collected from five distinct locations on each substrate using a 23.50 eV pass energy under ultra-high vacuum conditions. For the survey, N1s, and Ag 3d regions, we collected 7, 30, and 20 sweeps, respectively. The resulting spectra were summed together after calibration to the Ag 3d peak at 368.26 eV and Au 4f peak at 83.98 eV.[8] Then, the summed spectra were also calibrated with the same peaks. XPS spectra were processed using a linear,[8] Shirley,[9] or Tougaard[10] background subtraction, and peak fitting was performed using a Voigt peak shape in CasaXPS.[9] The Handbook of X-ray Photoelectron Spectroscopy,[11] CasaXPS software, and previous studies of NHC monolayers on gold[12] were used to interpret XPS data.

Scanning Electron Microscopy (SEM). To investigate and compare the etching behavior of Ag and Au surfaces, four different configurations of mirrors were prepared, each with a 5 nm thick chromium adhesion layer. (1) A purely Ag mirror, (2) a bilayer mirror consisting of an Ag layer deposited over an Au layer, (3) a bilayer consisting of an Au layer (~25nm) deposited over an Ag layer, and (4) a patterned mirror comprising stripes of Ag and Au. All prepared samples were subjected to heated methanolic deposition at 58 °C for 24 hours, and their subsequent morphological changes were characterized using scanning electron microscopy (SEM). SEM images were obtained using a Magellan 400 field-emission scanning electron microscope (FESEM) from Thermo Fisher Scientific. Aluminum stubs were used to mount the samples. The images were taken using a backscattered electron detector or a secondary electron detector.

Computational details. All calculations were carried out with a local modified version of the Amsterdam Density Functional (ADF) engine from Amsterdam Modeling Suite.[13] To model the SERS of NHC on Ag surface, a 58-atom silver cluster was used with the NHCs bound onto the adatom. For density functional theory (DFT) calculations, a Becke-Perdew (BP86) exchange-correlation functional[14, 15] in combination with Grimmes3 BJDAMP dispersion correction.[16] Geometry optimization of the NHC-Ag systems was performed with constraints that only allow the relaxation of the NHC molecule and the adatom. To filter out the influence of vibrations of the Ag cluster, a mobile block Hessian was calculated based on the optimized geometry.[17, 18] The frequencies and normal modes were calculated based on harmonic approximation. The Raman intensities were calculated from the squared polarizability derivatives with respect to normal mode displacements,[19] where the polarizabilities were calculated using the AOResponse module from ADF[20] with adiabatic local density approximation (ALDA) at the static limit. Based on the surface selection rules of SERS,[21-23] only the polarizability derivative components that are perpendicular to the Ag surface were included in the Raman intensity calculation. All images of the model systems were plotted with PyMol.[24](cite13)

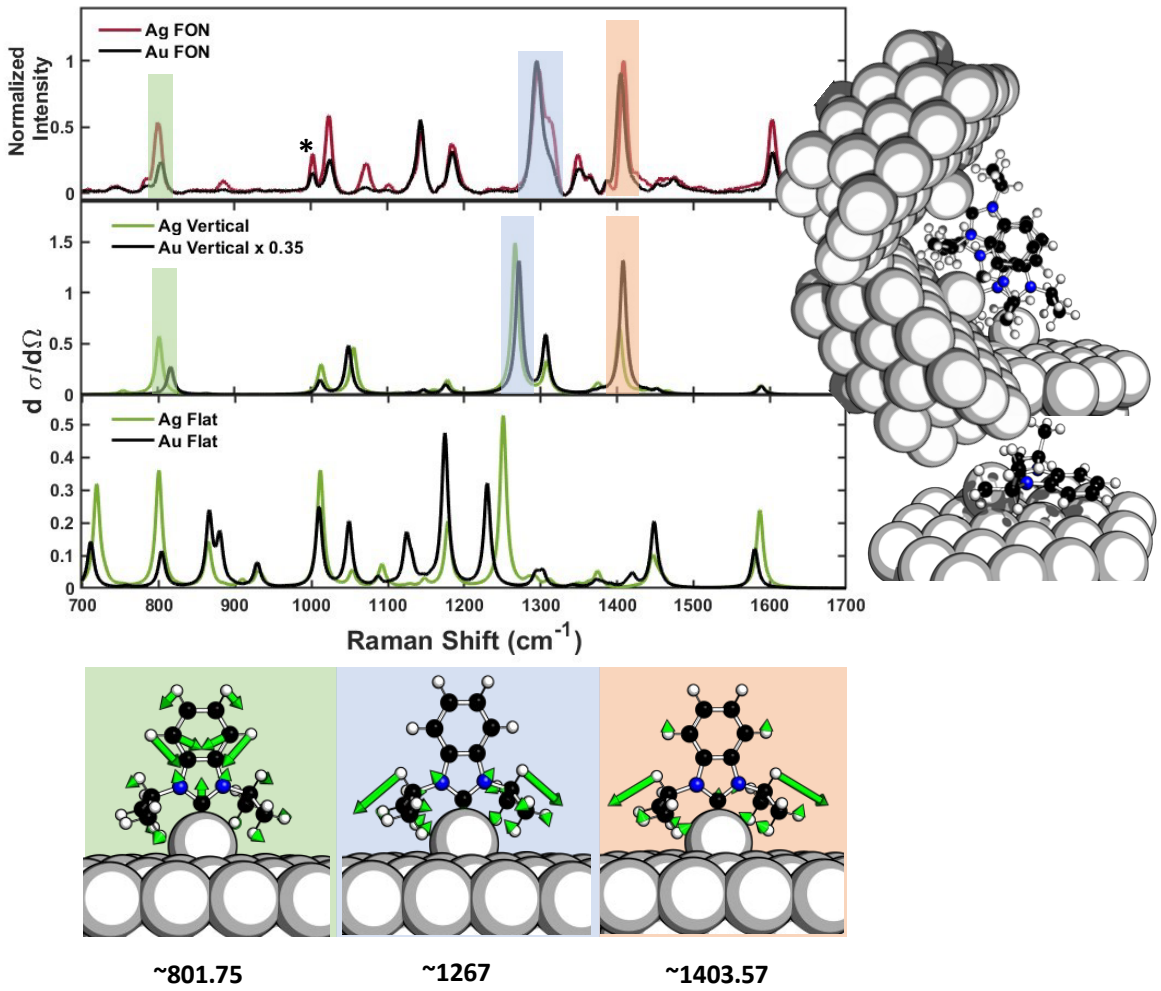

Figure S1. Experimental SERS spectra (top) of NHC-functionalized Au and Ag FONs. Simulated spectra of the ligand oriented vertically (middle) and flat (bottom) on the surface for each metal can be combined to predict the experimental spectra. The normal mode images at three frequencies are shown below, corresponding to the peaks that show the isotopic effect, highlighted in green, blue, and orange. The asterisk indicates the peak due to polystyrene beads below the silver or gold film.

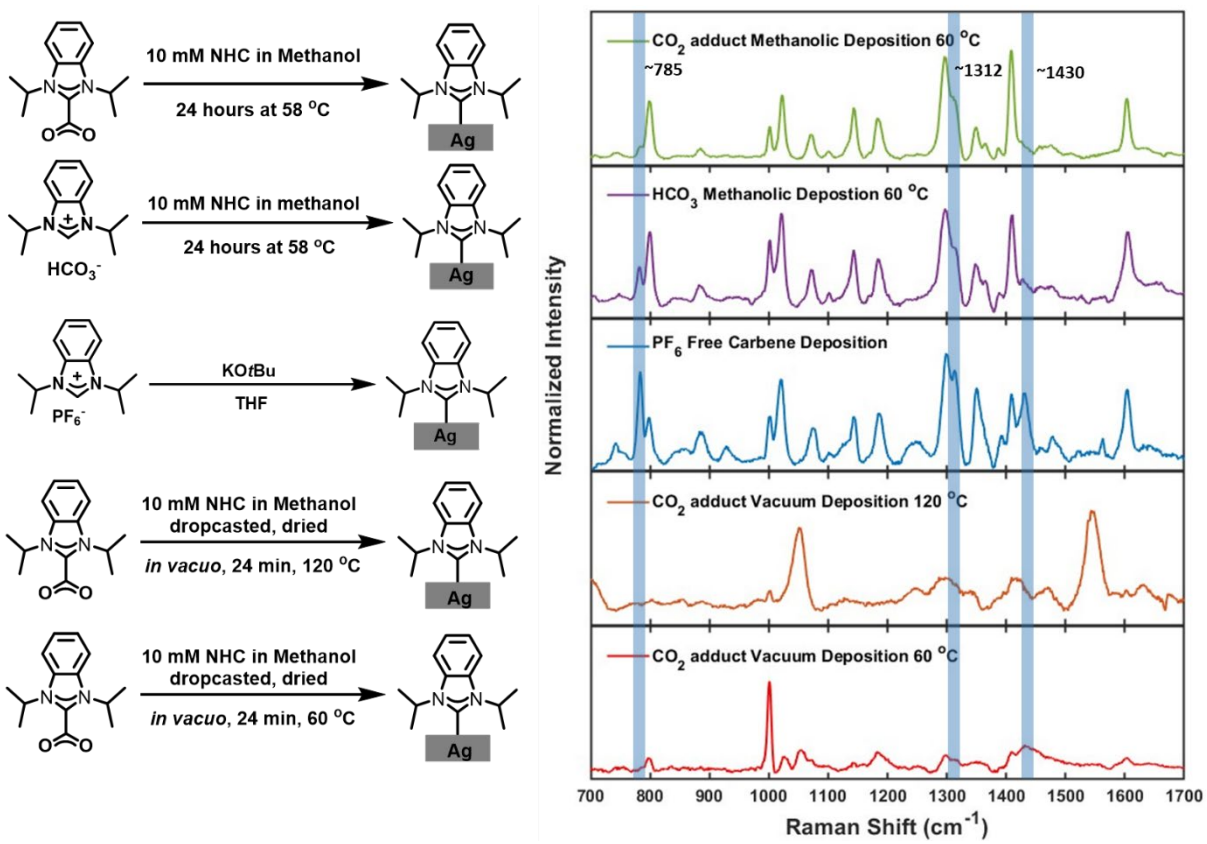

Figure S2. Resultant SERS of the NHC on the Ag surface from three different deposition protocols followed in this work. The blue highlights indicate the additional peaks observed for the methanolic deposition of **[(NHC-H)HCO_3]** and the free carbene method of **[(NHC-H)PF_6]**, suggesting that the surface structure is different.

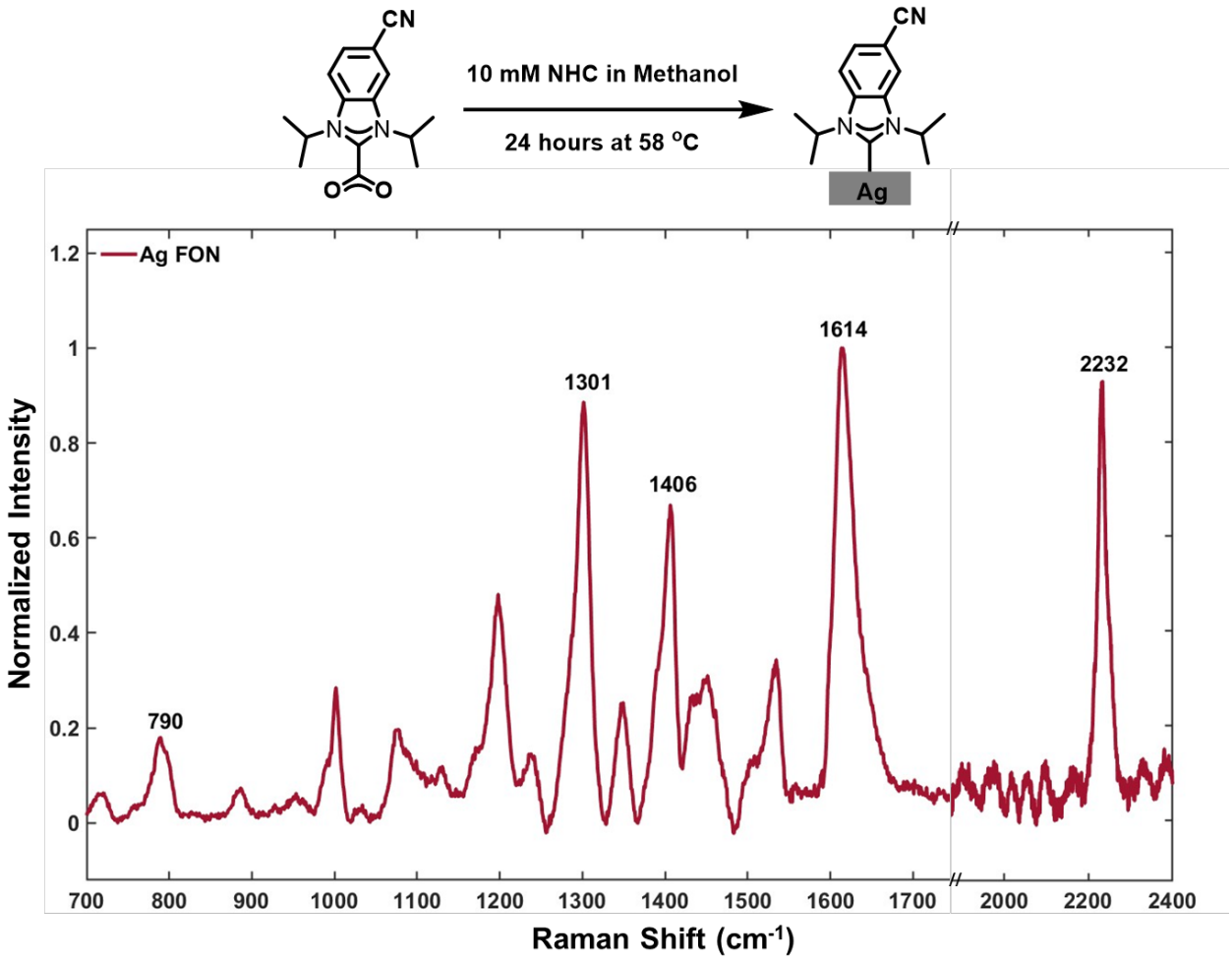

Figure S3. SERS of a benzimidazolium isopropyl NHC with a nitrile group attached to the 5' carbon after it was deposited on an Ag FON. This demonstrates that the heated methanolic deposition protocol is effective with different NHC ligands.

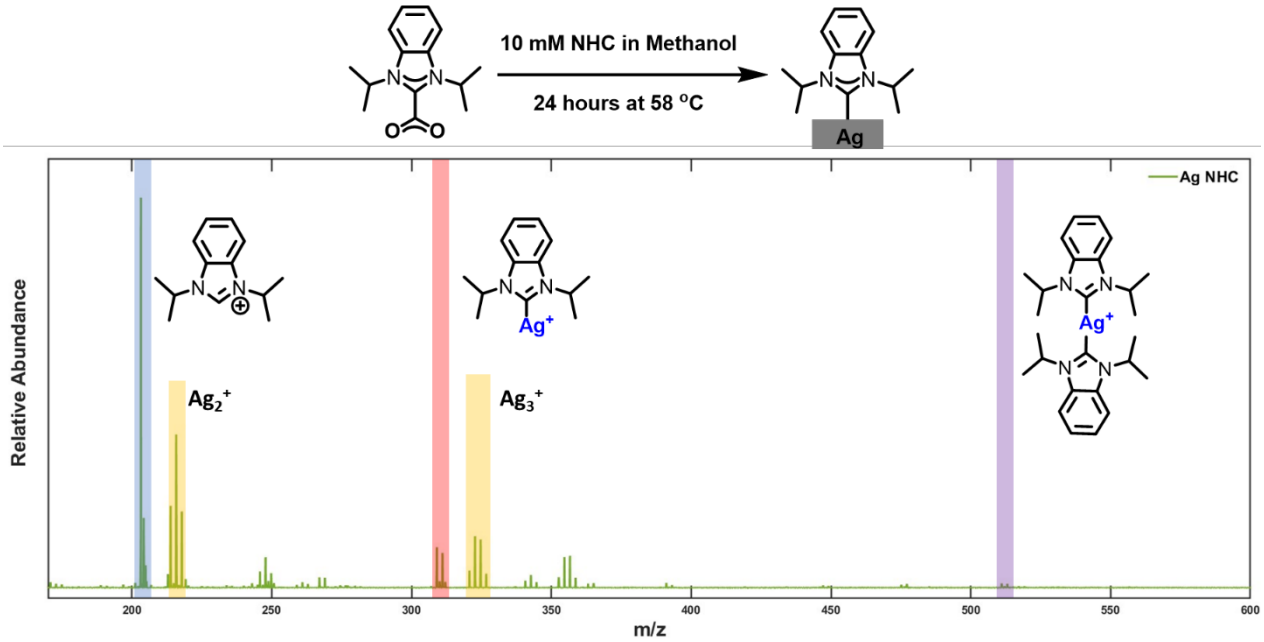

Figure S4. Full range of LDI-MS spectra from 150-600 m/z of NHC deposited on an Ag mirror.

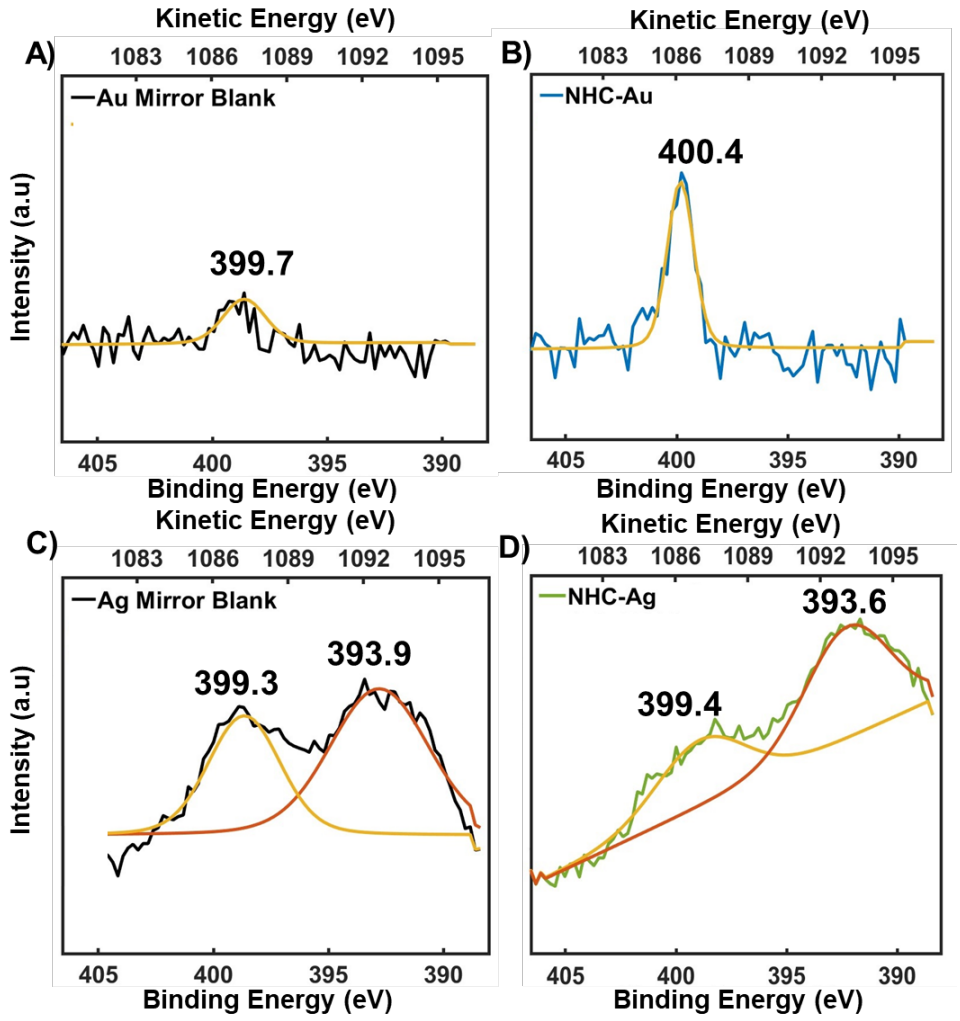

Figure S5. XPS N 1s elemental scans of Au and Ag mirrors. (A) and (C) shows the scans of Au and Ag mirrors subjected to deposition conditions without NHC ligands at 23 °C and 55 °C, respectively. (B) and (D) shows scans of Au and Ag mirrors subjected to heated methanolic deposition of **NHC-CO_2**. The presence of nitrogen peaks in the N 1s region of the Au mirror treated with methanol (A) indicates there may be trace nitrogen-containing organic impurities.[25, 26] The N 1s signal of the Au mirror subjected to NHC deposition is in agreement with the N 1s peak position of NHC-Au systems between 399.9 and 401.0 eV.[27] For the silver mirror subjected to deposition, although the N1s peaks fall in a similar region, the Ag mirror control shows a similar peak. As reported in previous studies, the peak at 399.3 eV corresponds to the energy loss from Ag $3d_{5/2,}$ and the peak at 393.9 eV corresponds to Ag $3d_{3/2}$.[28] The data in (A) and (B) are reproduced from Ref-30.

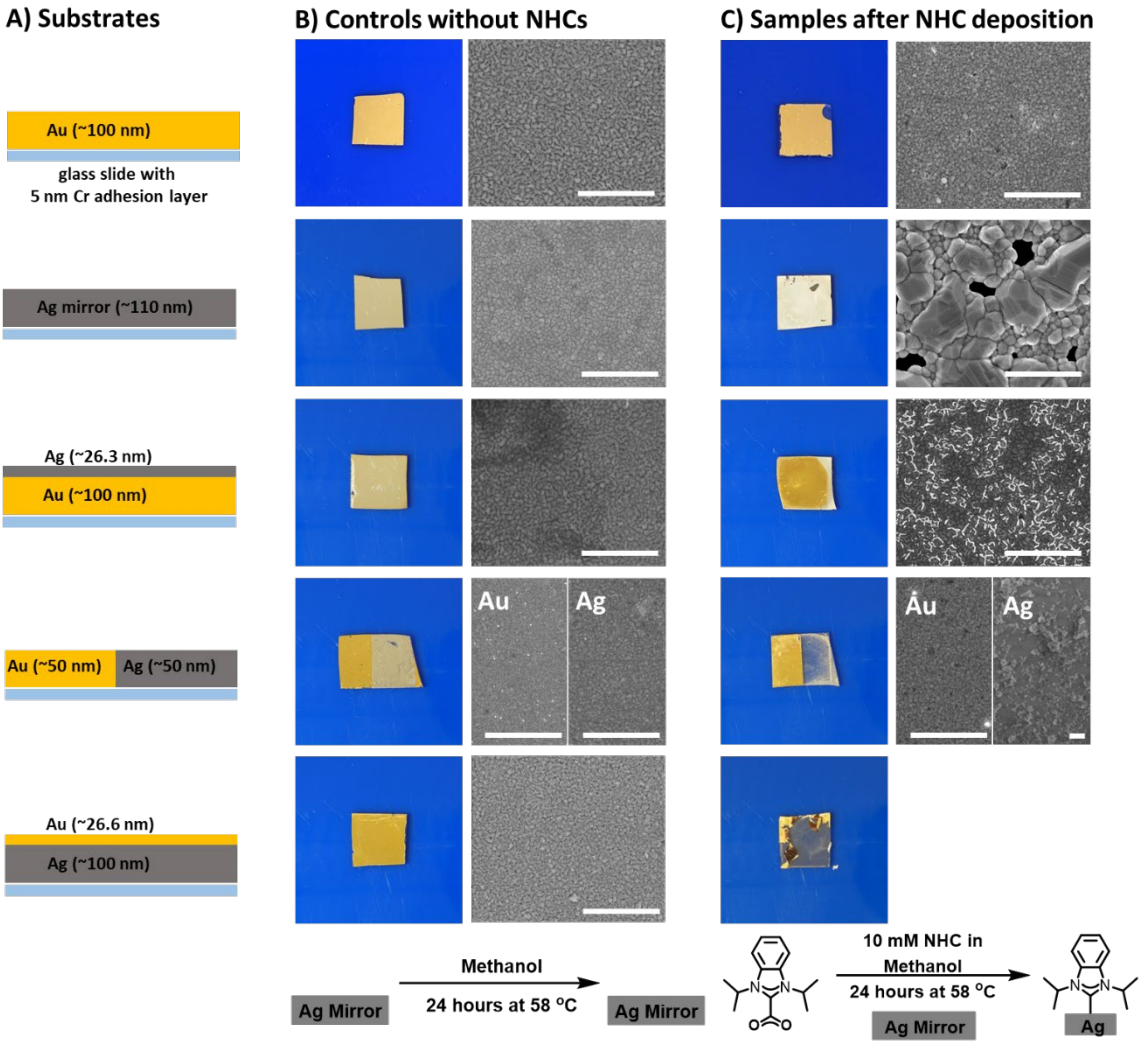

Figure S6. SEM of NHCs deposited on Ag and Au substrates (A), photographs and SEM images of the substrates without (B) and with (C) NHCs. This figure is an expansion of Figure 5 to include the Au mirror control (top) and an Ag mirror coated with a thin layer of Au (bottom). The length of the scale bars represents 1 μm.

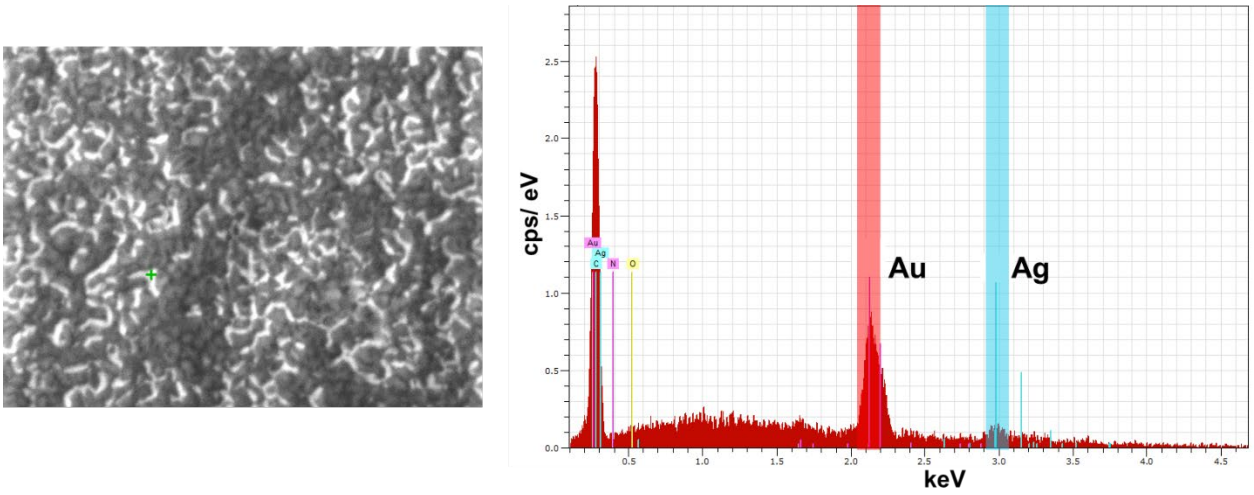

Figure S7. SEM-EDX of the remaining Ag on top of Au after methanolic deposition resulted in the etching of a bilayer of Au (~100 nm) with Ag (~25 nm) on top.

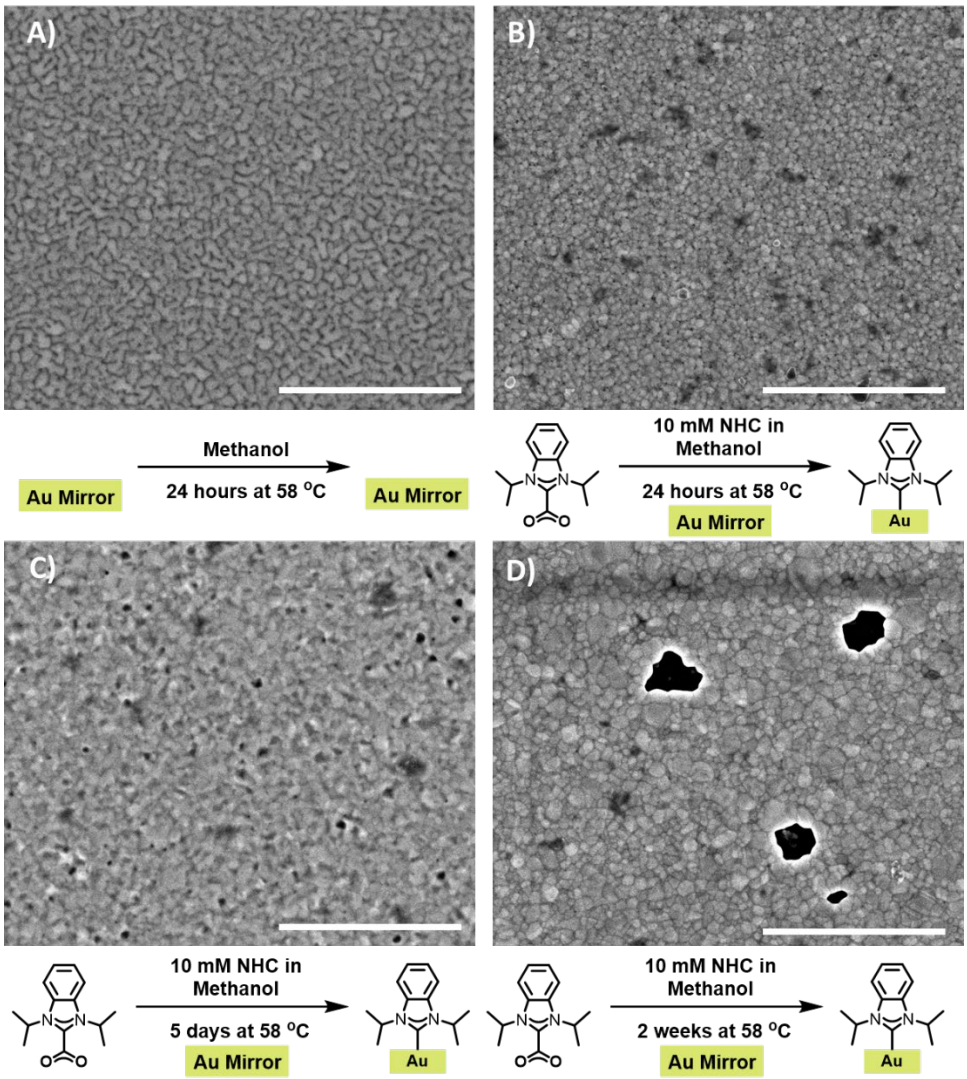

Figure S8. SEM of Au mirrors subjected to an extended period of heated methanolic deposition. (A) Au mirror subjected to heated methanolic deposition conditions without NHCs. (B), (C), and (D) shows the Au mirror subjected to heated methanolic deposition of NHC-CO2 adduct for 24 hours, 5 days, and two weeks, respectively. With extended time, etching of the Au surface is visible on the SEM images. The length of the scale bar represents 1 μm.

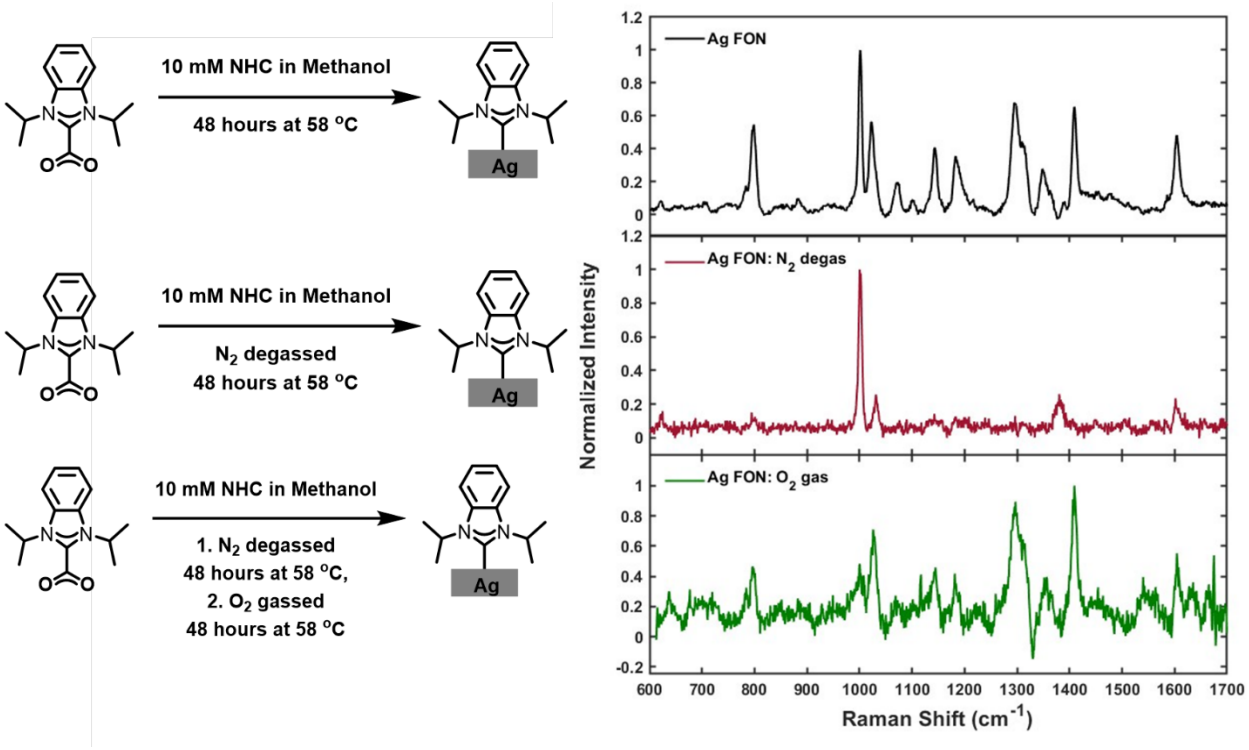

Figure S9. Comparison of the SERS of NHC on Ag with deposition performed using regular methanol (top), with methanol degassed with nitrogen to get rid of dissolved oxygen (middle), and after oxygen was redissolved into the methanol (bottom).

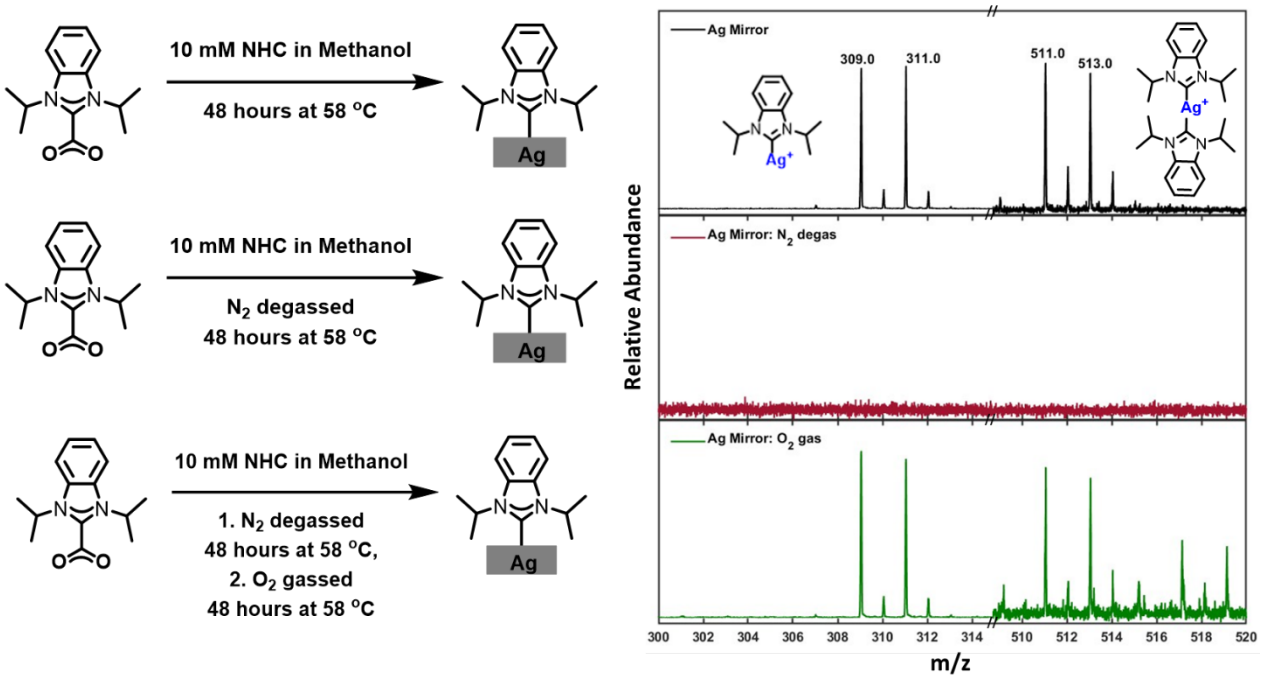

Figure S10. Comparison of the LDI-MS of NHC on Ag with deposition performed using regular methanol (top), with methanol degassed with nitrogen to get rid of dissolved oxygen (middle), and after oxygen was redissolved into the methanol (bottom)

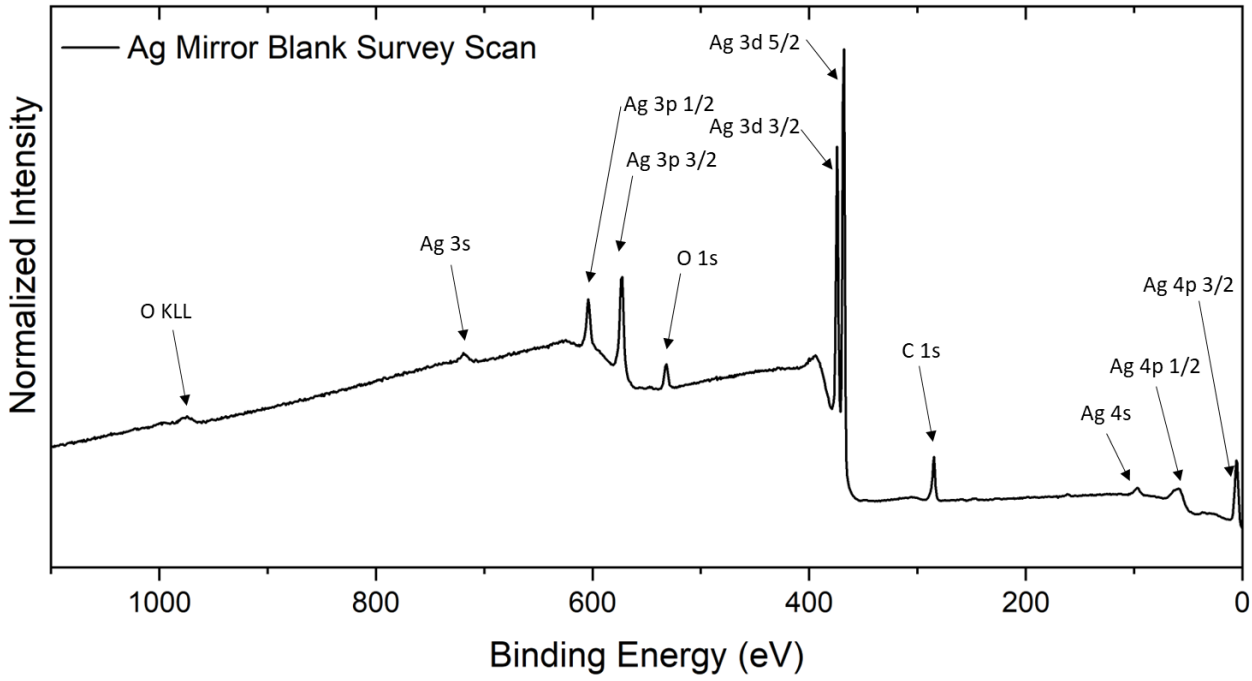

Figure S11. XPS survey scan Ag Mirror subjected to heated methanolic deposition at 55 °C for 24 hours without NHC ligands.

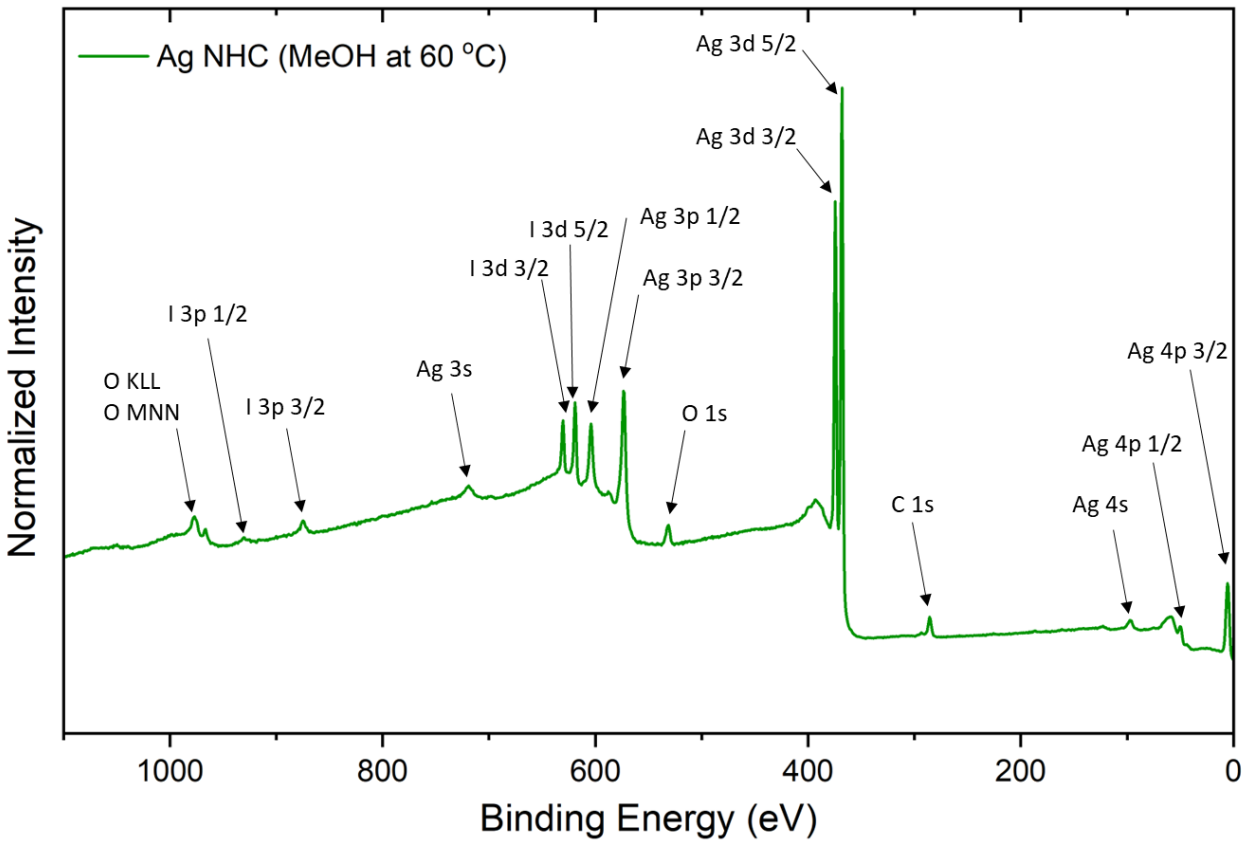

Figure S12. XPS survey scan Ag Mirror subjected to heated methanolic deposition of **NHC-CO_2** at 55 °C for 24 hours. Iodine was observed in the XPS spectra, which has been observed in previous studies of the NHC monolayers on gold.[29, 30]

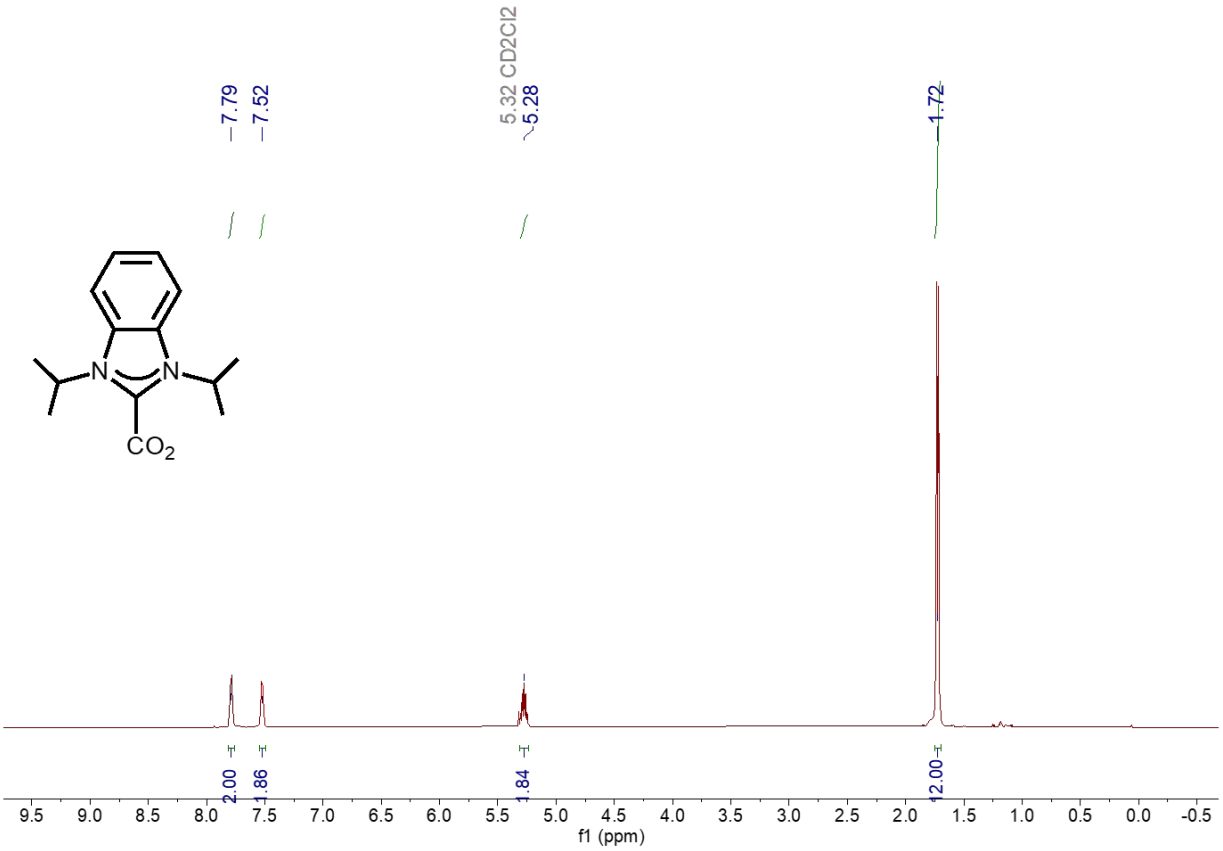

Figure S13. ^{1}H NMR spectrum of NHC-CO_2 adduct in CD_2Cl_2.

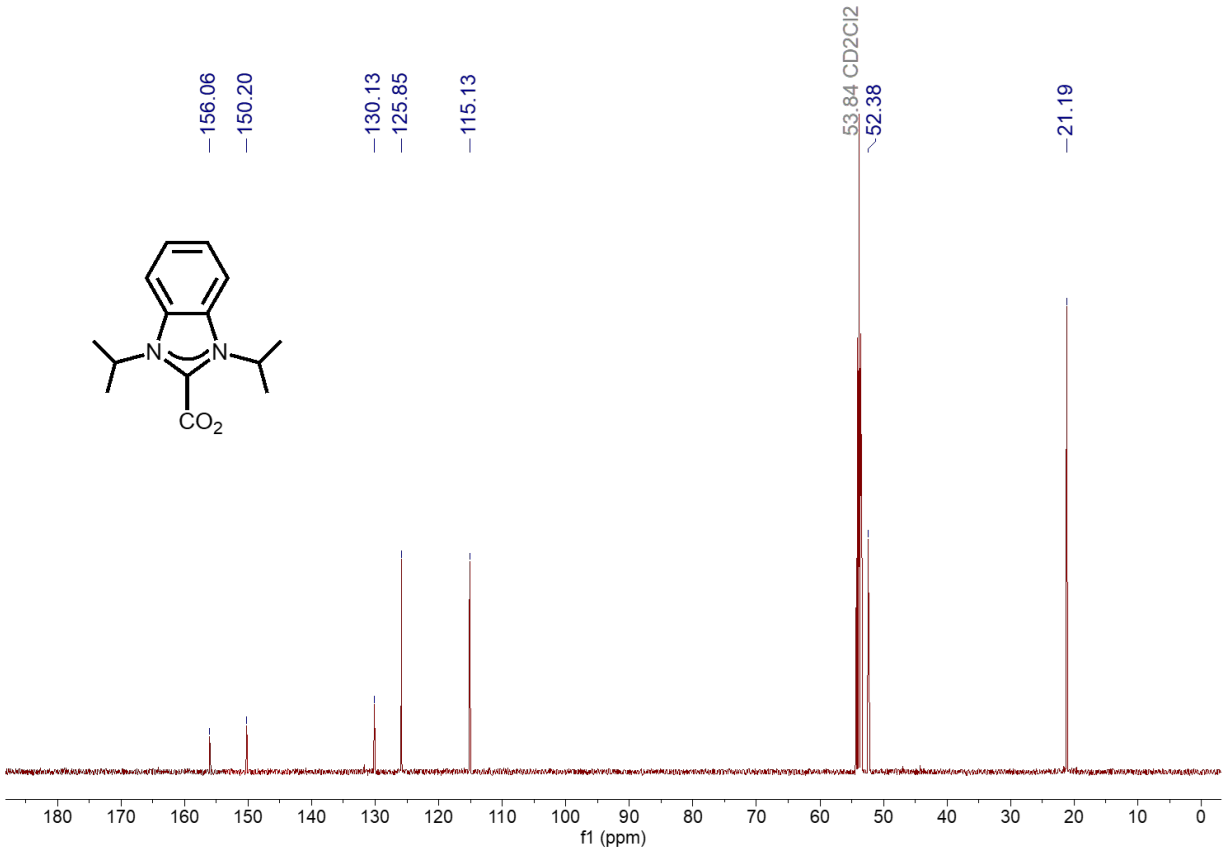

Figure S14. $^{13}C\{^{1}H\}$ NMR spectrum of NHC-CO_2 adduct in CD_2Cl_2.

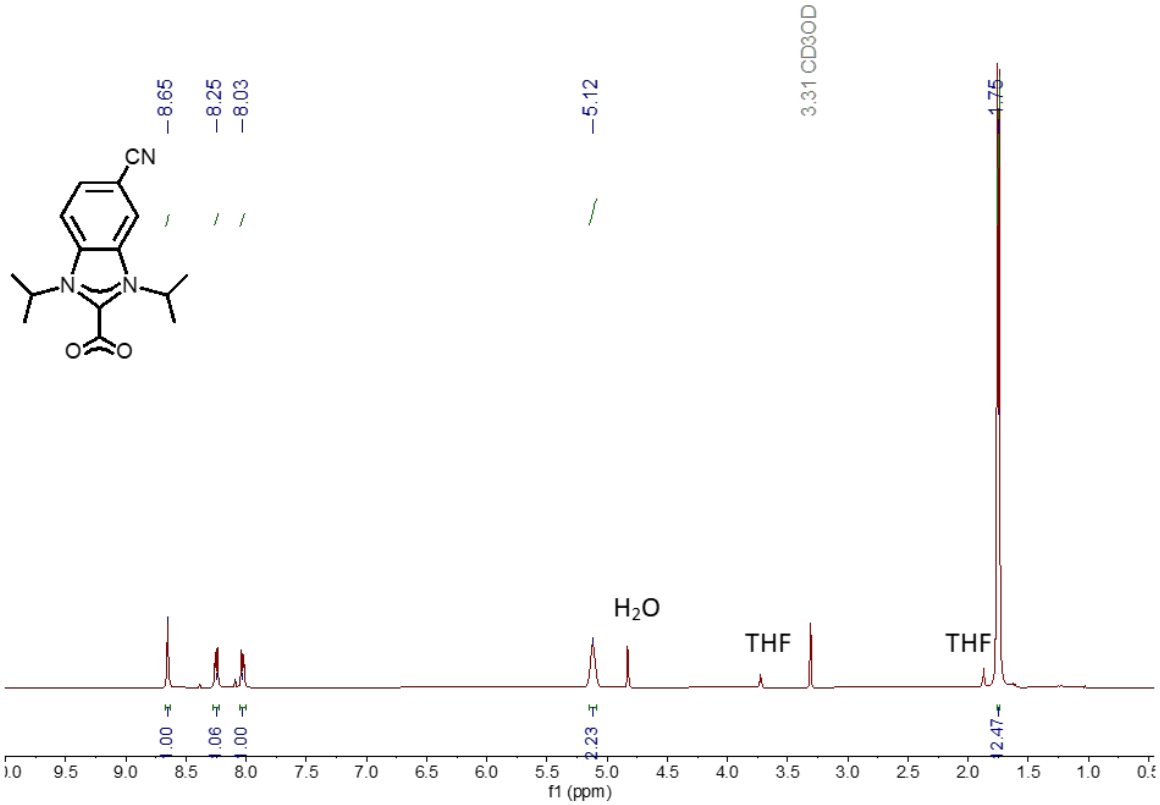

Figure S15. ^{1}H NMR spectrum of NHC-CO_2 adduct with CN backbone in CD_3OD.

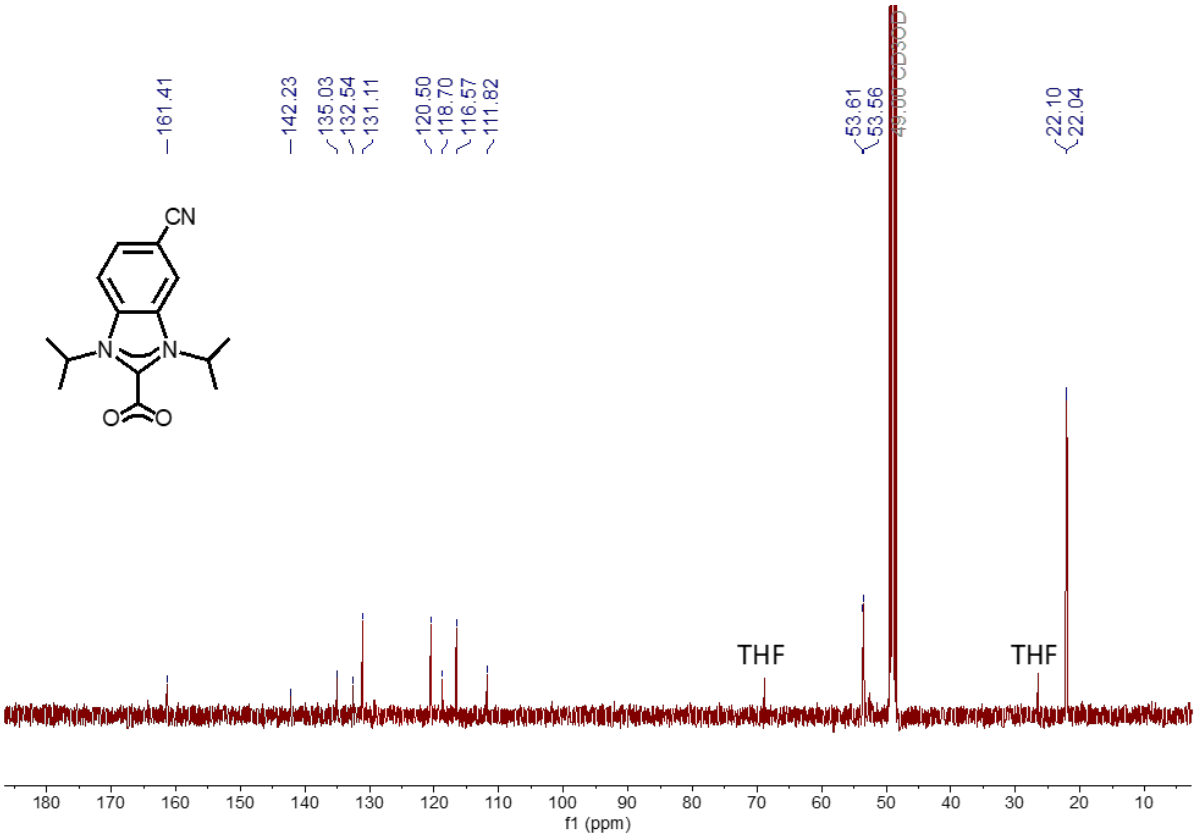

Figure S16. ^{13}C { ^{1}H} NMR spectrum of NHC-CO_2 adduct with CN backbone in CD_3OD.

References

1. J. F. DeJesus, M. J. Trujillo, J. P. Camden and D. M. Jenkins, *Journal of the American Chemical Society*, 2018, **140**, 1247-1250.

2. S. J. Lee, Z. Guan, H. Xu and M. Moskovits, *The Journal of Physical Chemistry C*, 2007, **111**, 17985-17988.

3. J. F. DeJesus, L. M. Sherman, D. J. Yohannan, J. C. Becca, S. L. Strausser, L. F. P. Karger, L. Jensen, D. M. Jenkins and J. P. Camden, *Angew Chem Int Ed*, 2020, **59**, 7585-7590.

4. L. M. Sherman, S. L. Strausser, R. K. Borsari, D. M. Jenkins and J. P. Camden, *Langmuir*, 2021, **37**, 5864-5871.

5. M. J. Trujillo, S. L. Strausser, J. C. Becca, J. F. DeJesus, L. Jensen, D. M. Jenkins and J. P. Camden, *J Phys Chem Lett*, 2018, **9**, 6779-6785.

6. N. L. Dominique, A. Chandran, I. M. Jensen, D. M. Jenkins and J. P. Camden, *Chemistry – A European Journal*, 2024, **30**, e202303681.

7. L. Kolarova, L. Prokes, L. Kucera, A. Hampl, E. Pena-Mendez, P. Vanhara and J. Havel, *J Am Soc Mass Spectrom*, 2017, **28**, 419-427.

8. A. G. Shard, *J Vac Sci Technol A*, 2020, **38**, 041201.

9. G. H. Major, N. Farley, P. M. A. Sherwood, M. R. Linford, J. Terry, V. Fernandez and K. Artyushkova, *J Vac Sci Technol A*, 2020, **38**, 061203.

10. S. Tougaard, *Surf Sci*, 1989, **216**, 343-360.

11. J. F. Moulder and J. Chastain, *Handbook of x-ray photoelectron spectroscopy : a reference book of standard spectra for identification and interpretation of XPS data*, Eden Prairie, Minn. : Physical Electronics Division, Perkin-Elmer Corp., 1992.

12. A. Inayeh, R. R. K. Groome, I. Singh, A. J. Veinot, F. C. de Lima, R. H. Miwa, C. M. Crudden and A. B. McLean, *Nat. Commun.*, 2021, **12**, 4034.

13. G. t. Te Velde, F. M. Bickelhaupt, E. J. Baerends, C. Fonseca Guerra, S. J. van Gisbergen, J. G. Snijders and T. Ziegler, *Journal of Computational chemistry*, 2001, **22**, 931-967.

14. A. D. Becke, *Physical review A*, 1988, **38**, 3098.

15. J. P. Perdew, *Physical review B*, 1986, **33**, 8822.

16. S. Grimme, S. Ehrlich and L. Goerigk, *Journal of computational chemistry*, 2011, **32**, 1456-1465.

17. A. Ghysels, D. Van Neck, V. Van Speybroeck, T. Verstraelen and M. Waroquier, *The Journal of chemical physics*, 2007, **126**.

18. A. Ghysels, D. Van Neck and M. Waroquier, *The Journal of chemical physics*, 2007, **127**.

19. J. Neugebauer, M. Reiher, C. Kind and B. A. Hess, *Journal of computational chemistry*, 2002, **23**, 895-910.

20. L. Jensen, L. Zhao, J. Autschbach and G. Schatz, *The Journal of chemical physics*, 2005, **123**.

21. E. Le Ru, S. Meyer, C. Artur, P. Etchegoin, J. Grand, P. Lang and F. Maurel, *Chemical Communications*, 2011, **47**, 3903-3905.

22. M. Moskovits and J. Suh, *The Journal of Physical Chemistry*, 1984, **88**, 5526-5530.

23. M. Moskovits, *The Journal of Chemical Physics*, 1982, **77**, 4408-4416.

24. *The PyMOL Molecular Graphics System, Version 3.0; Schrödinger, LLC*.

25. G. Guella, D. Ascenzi, P. Franceschi and P. Tosi, *Rapid Communications in Mass Spectrometry: An International Journal Devoted to the Rapid Dissemination of Up-to-the-Minute Research in Mass Spectrometry*, 2007, **21**, 3337-3344.

26. B. Deshmukh and J. Coetzee, *Analytical Chemistry*, 1984, **56**, 2373-2378.

27. A. Inayeh, R. R. Groome, I. Singh, A. J. Veinot, F. C. de Lima, R. H. Miwa, C. M. Crudden and A. B. McLean, *Nature Communications*, 2021, **12**, 4034.

28. N. Pauly, F. Yubero and S. Tougaard, *Applied surface science*, 2016, **383**, 317-323.

29. A. Krzykawska, M. Wrobel, K. Kozieł and P. Cyganik, *ACS nano*, 2020, **14**, 6043-6057.

30. A. Chandran, N. L. Dominique, G. Kaur, V. Clark, P. Nalaoh, L. C. Ekowo, I. M. Jensen, M. D. Aloisio, C. M. Crudden, N. Arroyo-Currás, D. M. Jenkins and J. P. Camden, *Nanoscale*, 2025, **17**, 5413-5428.